Zhao Y, Lu J, Zhang Y, Wu F, Huo D. Development of an analytical model based on Mohr–Coulomb criterion for cutting of metallic glasses. *International Journal of Mechanical Sciences* 2016, 106, 168-175.

Development of an analytical model based on Mohr–Coulomb criterion for cutting of metallic glasses

Yan Zhao, Jingping Lu, Yan Zhang, Fenghe Wu, Dehong Huo

www.elsevier.com/locate/ijmecsci

PII: S0020-7403(15)00443-9
DOI: http://dx.doi.org/10.1016/j.ijmecsci.2015.12.016
Reference: MS3180

To appear in: *International Journal of Mechanical Sciences*

Received date: 3 August 2015
Revised date: 30 November 2015
Accepted date: 21 December 2015

Cite this article as: Yan Zhao, Jingping Lu, Yan Zhang, Fenghe Wu and Dehong Huo, Development of an analytical model based on Mohr–Coulomb criterion fo cutting of metallic glasses, *International Journal of Mechanical Sciences* http://dx.doi.org/10.1016/j.ijmecsci.2015.12.016

Development of an analytical model based on Mohr–Coulomb criterion for cutting of metallic glasses

Yan Zhao[1], Jingping Lu[1], Yan Zhang[1], Fenghe Wu[1], Dehong Huo[2*]

[1]*School of Mechanical Engineering, Yanshan University, 066004, China*

[2]*School of Mechanical and Systems Engineering, Newcastle University, Newcastle Upon Tyne, NE7 7QH, UK*

[*]Corresponding author: Dehong Huo, Tel: +0044 191 208 6230; email: dehong.huo@ncl.ac.uk

Abstract

The tension-compression asymmetry of metallic glasses has shown that the Mohr-Coulomb yield criterion can better determine the fracture characteristics of metallic glasses than the traditional Tresca and Von Mises criterion. Available cutting models based on the traditional yield criterion cannot describe the cutting mechanism of metallic glasses. An orthogonal cutting mechanics model of metallic glasses based on the Mohr-Coulomb yield criterion taking into account the influence of normal stress and temperature on shear plane is established. The analytical expressions for cutting force, shear angle and average temperature rise on shear plane are derived. Orthogonal turning experiments were designed and carried to validate the developed model. The analytically calculated cutting forces from the developed model considering cutting temperature rise were compared with the measured forces and the results show that a small difference of 7.7% was found, which is contrary to the prediction from traditional model based on von Mises yield criterion (nearly 60%) and the prediction from the model based on M-C without considering cutting temperature rise (more than 70%). The comprehensive comparison results show that the developed analytical model can accurately predict cutting process for metallic glasses.

Keywords: analytical cutting model, Mohr-Coulomb failure criterion, orthogonal cutting, metallic glasses, cutting force, cutting temperature

Nomenclature

τ_n——shear yield stress on shear plane;

σ_n——normal stress on shear plane;

k——material cohesion strength;

λ——temperature influence coefficient;

T——resultant temperature on shear plane, $T=T_0+T_s$;

T_s——average temperature rise on shear plane;

T_0——room temperature;

T_g——glass transition temperature;

α——material internal coefficient;

t_1——uncut chip thickness;

t_2——chip thickness;

w——cutting width;

V——cutting velocity;

V_s——shear velocity on shear plane;

V_c——outflow velocity of chip

R'——resultant force on the shear plane acting on the workpiece;

R——resultant force on tool-chip interface acting on the tool;

F_n——normal force on shear plane;

F_s——shear force on shear plane;

F_f——friction force on tool-chip interface;

F_N——normal force on tool-chip interface;

N——normal force on flank acting by machined surface;

f——friction force on flank acting by machined surface;

φ——shear angle;

β——tool-chip friction angle;

γ——rake angle;

χ——inflow rate;

c——specific heat capacity;

ρ——density;

ξ——thermal conductivity;

n——spindle speed;

a_p——cutting depth;

f——feed rate;

d——actual cutting depth;

d_1——workpiece diameter before turning;

d_2——workpiece diameter after turning;

δ——cutting depth error;

Δ——relative cutting depth error;

F_x——feed force;

F_y——radial thrust force;

F_z——principle cutting force;

F_{y1}——component force of F_y on rake face and flank;

F_{y2}——component force of F_y at connection surface of flank and vice flank

1. Introduction

Bulk metallic glasses (BMGs) as new engineering materials exhibit excellent mechanical, physical and chemical properties over traditional metals, such as high yield strength (~2 GPa) and elastic limit(~2%) as reported by Lee *et al*. (2005), due to their long-range disorder and short-range order microstructure. However, Zhang *et al*. (2003a) and Liu (2005) have found that BMGs undergo little plastic deformation before fracture and the plastic deformation usually occurs on one dominant shear band at room temperature. Zhang, *et al*. (2003b) and Chen *et al*. (2012) conducted the tension and compression tests of BMGs and classified them as pressure sensitive materials, for example, the compressive strength is usual greater than tensile strength , also the yield asymmetry of tension and compression is affected by temperature.

Cutting is one of the most basic processes for shaping BMG parts with high dimensional accuracy and surface roughness requirements. Bakkal *et al*. (2004) investigated the chip light emission and morphology, cutting forces, surface roughness, and tool wear in turning of Zr-based BMG together with an Al alloy and SUS304 stainless steel under the same cutting condition using the different tool materials. Fujita *et al*. (2005) reported the cutting characteristics in turning BMGs with different tool materials, nose radii and cutting speeds. These work experimentally demonstrated the machinability of BMGs and investigated the influence of cutting parameters and tool geometry on the machining quality of BMGs.

In order to further study the cutting mechanism, Jiang and Dai (2009) developed a coupled thermomechanical orthogonal cutting model to quantitatively characterize lamellar chip formation. More recently, Ye *et al*. (2012) proposed a new slip-line field model for orthogonal cutting of pressure sensitive materials and the analytical expressions for shear angle, cutting force, and chip configuration were given. The authors believed that the slip-line field model can better describe the deformation process in cutting BMGs. However temperature rise was not taken into consideration in their FEM model and the results have not been validated by experiments. On the other hand, due to the fact that BMGs are temperature sensitive materials and their material properties are strongly affected by temperature, it is necessary to include the temperature effect in the model. Nevertheless, these research results have laid the foundation for the research of the cutting mechanism of metallic glasses.

Cutting process can be characterized by its high stresses, high strain and strain rate, high temperature rise, and unusual frictional conditions. Available cutting models based on the Tresca or von Mises yield criterion do not consider the effects of hydrostatic pressure and temperature rise on cutting forces in cutting process. However the yield strength of metallic glasses is sensitive to hydrostatic pressure and temperature, and hence should be included in the modelling. This paper aims to establish an orthogonal cutting mechanics model of metallic glasses based on the M-C yield criterion which takes into account the pressure and temperature on the shear plane. A geometric orthogonal cutting model was first established, and then the analytical expressions for cutting force, shear angle and temperature were

derived accordingly. Finally, the cutting experiments were carried out to verify the cutting model developed.

2. Orthogonal cutting mechanics model

2.1 Yield criterion

The yield criterion is the theoretical basis of the establishment of cutting model. Materials in cutting process generally undergo a transition from elastic to plastic state, and the yield criterion is the quantitative description when the material reaches the critical plastic condition. Lund and Schuh (2004) and Zhang (2003a) found that Mohr-Coulomb criterion that can describe the deformation characteristics of the pressure sensitive materials and it is a better description of the yielding behavior of metallic glasses than the classical von Mises or Tresca criteria used widely in crystalline metal materials, because both von Mises and Tresca criteria cannot describe the influence of hydrostatic pressure on the shear plane of metallic glasses. In fact, many tension and compression tests showed that the metallic glasses are the pressure and temperature sensitive materials. So, Sun et al. (2010) established the comprehensive yield criterion considering the metallic glass pressure sensitive effect and temperature effect. However, it is difficult to obtain the value of some parameters in Sun's criterion in practice. Based on the M-C criterion and adding the temperature function item to it, Chen, et al. (2012) gave the expression of shear yield stress:

$$\tau_n = k \cdot \left(1 - \sqrt{\lambda \cdot T / T_g}\right) + \alpha \cdot \sigma_n \tag{1}$$

where τ_n is the shear yield stress on shear plane, k is material cohesion strength, λ is temperature influence coefficient, T is the resultant temperature on shear plane, T_g is the glass transition temperature, α is the material internal friction coefficient that dictates the strength of the normal stress dependence, and σ_n is the stress normal to the shear plane. Eq(1) shows that a temperature rise will reduce shear yield stress whilst an increase of normal stress σ_n will have an opposite effect on it. The analytical cutting force model established in this paper was based on Eq(1).

2.2 Establishment of the orthogonal cutting geometry model

Before the establishment of the orthogonal cutting model the cutting conditions are simplified in order to avoid the complex calculation process. Four premises are made as follows:

1) *Thin shear zone*. When the material yields, the plastic deformation in primary shear zone is assumed to be concentrated along a single shear plane;
2) *Frictional conditions on the tool*. Tool wear is ignored. The friction and pressure on the flank of tool is considered, and the friction condition on the rake face and the flank are assumed to be Coulomb friction. After the turning experiments of metallic glasses, it was found that the flank wore greatly.
3) *Plane strain state*. The cutting width is assumed far greater than the thickness of cutting, therefore, the plastic deformation occurring in the plane perpendicular to the cutting edge is the same;
4) *Shear zone stress distribution*. Normal stress and shear stress on the shear plane is uniformly distributed.

Thus, the orthogonal cutting geometry model for cutting metallic glass materials which is based on Merchant model and meets the above four premises can be established as shown in Fig. 1. As it can be seen from Fig. 1, the tool is subjected to the friction and pressure from the rake face and the flank face at same time. The shear slip followed by the materials yielding occurs entirely across the shear line *AB*. The chip is at static equilibrium under the action of two resultant forces *R'* and *R* which are from the workpiece and the rake face, respectively.

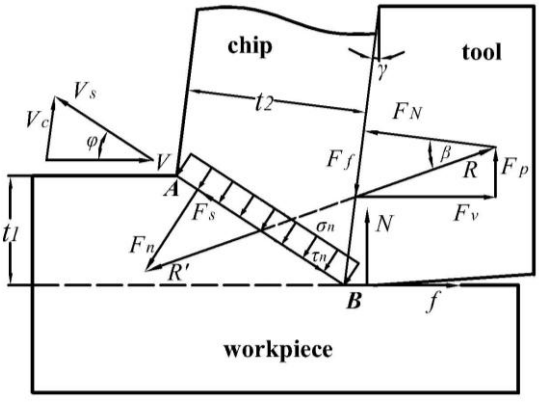

Fig. 1 The orthogonal cutting geometry model for cutting metallic glass materials

2.3 Analytical expressions

2.3.1 Cutting force

Here, we consider that the shear stress on the shear plane is equal to the yield strength of the material. According to the above geometric model, the shear force F_s on the shear plane is obtained by:

$$F_s = \frac{\tau_n \cdot t_1 \cdot w}{\sin\varphi} \tag{2}$$

where t_1 is the uncut chip thickness, w is the cutting width, and φ is the shear angle.

The resultant force R' acting on the shear plane can be expressed as

$$R' = \frac{F_s}{\cos(\varphi+\beta-\gamma)} = \frac{\tau_n \cdot t_1 \cdot w}{\sin\varphi \cdot \cos(\varphi+\beta-\gamma)} \tag{3}$$

where β and γ is the tool-chip friction angle and the tool rake angle respectively.

By the geometric relationship on the shear plane in Fig. 1, the normal stress σ_n can be expressed as

$$\sigma_n = \tan(\varphi+\beta-\gamma)\cdot\tau_n \tag{4}$$

Here, the expression of shear stress can be transformed into another form by substituting the Eq(4) into the Eq(1)

$$\tau_n = \frac{k\cdot\left(1-\sqrt{\lambda\cdot T/T_g}\right)}{1-\alpha\cdot\tan(\varphi+\beta-\gamma)} \tag{5}$$

By the static equilibrium condition of the chip, the magnitude of the two forces R' and R is equal, the analytical expression for R by substituting the Eq(5) into the Eq(3) can be obtained as:

$$R = \frac{k\cdot\left(1-\sqrt{\lambda\cdot T/T_g}\right)\cdot t_1\cdot w}{[1-\alpha\cdot\tan(\varphi+\beta-\gamma)]\sin\varphi\cdot\cos(\varphi+\beta-\gamma)} \tag{6}$$

Analyzing the forces of tool in Fig. 1, the resultant force R can be decomposed into two orthogonal component force F_v and F_p, acting along the cutting velocity and perpendicular to the cutting velocity respectively. Their expressions are:

$$\left.\begin{aligned} F_v &= R\cdot\cos(\beta-\gamma) \\ F_p &= R\cdot\sin(\beta-\gamma) \end{aligned}\right\} \tag{7}$$

By substituting Eq(6) into Eq(7), the analytical expression for the force F_v and F_p can be obtained

$$F_v = \frac{k\cdot\left(1-\sqrt{\lambda\cdot T/T_g}\right)\cdot t_1\cdot w\cdot\cos(\beta-\gamma)}{\left[1-\alpha\cdot\tan(\varphi+\beta-\gamma)\right]\cdot\sin\varphi\cdot\cos(\varphi+\beta-\gamma)} \tag{8}$$

$$F_p = \frac{k\cdot\left(1-\sqrt{\lambda\cdot T/T_g}\right)\cdot t_1\cdot w\cdot\sin(\beta-\gamma)}{\left[1-\alpha\cdot\tan(\varphi+\beta-\gamma)\right]\cdot\sin\varphi\cdot\cos(\varphi+\beta-\gamma)} \tag{9}$$

Eq(8) and (9) show that both cutting forces decreases with the increase of the temperature T on the shear plane, but increases with the increase of the material internal friction coefficient α. The influence of the shear angle φ on the cutting force is not very intuitive, but it can be determined through the numerical fitting. Figure 2 shows the result of the numerical fitting between the shear angle φ and the cutting force F_v in Eq(8) where all physical quantities are set as constants except the shear angle φ. The curve shows that the shear angle φ and the cutting force F_v have a relationship similar to a quadratic function. No matter how other parameters change, there exists a specific shear angle at which the cutting force reaches the minimum.

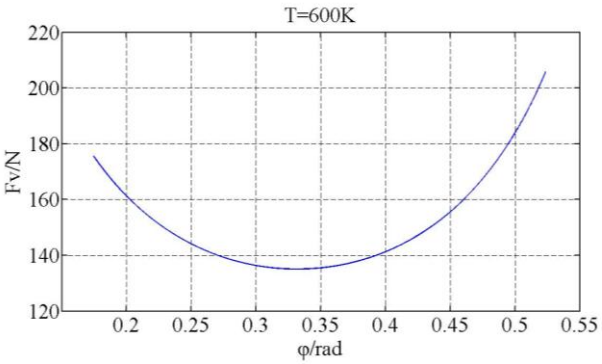

Fig. 2 The numerical fitting curve of the shear angle φ and the cutting force F_v

(Parameters used: k = 1GPa, $t_1 \cdot w$ = 0.036mm^2, β-γ = π/4, λ = 0.2, α = 0.123, T_g=638K, material: Vit1 metallic glass (refer to Table 1 for material properties))

2.3.2 Shear angle

The shear angle is the angle between the direction of cutting velocity and the shear plane. Although at present there is not an accurate method to theoretically predict the shear angle without relying on cutting experiments, the minimum energy principle proposed by Merchant (1945a) that the shear angle is when the minimum energy is consumed in the cutting process is a widely employed method. The curve in Fig. 2 also illustrates this principle. According to this principle, the cutting energy per unit volume, P_v, is obtained as

$$P_v = \frac{F_v \cdot V}{V \cdot t_1 \cdot w} = \frac{k \cdot \left(1 - \sqrt{\lambda \cdot T / T_g}\right) \cdot \cos(\beta - \gamma)}{\left[1 - \alpha \cdot \tan(\varphi + \beta - \gamma)\right] \cdot \sin\varphi \cdot \cos(\varphi + \beta - \gamma)} \tag{10}$$

By taking the partial derivative of the cutting energy Eq(10) and set the derivation results equal to zero, i.e. $dP_v/d\varphi = 0$, the cutting energy reaches the minimum. So the expression for the shear angle φ can be predicted:

$$\varphi = \frac{1}{2}\left[\arctan\frac{1}{\alpha} - (\beta - \gamma)\right] \tag{11}$$

As can be known from the Eq(11), the shear angle φ increases with the increase of the rake angle γ, but decreases with the increase of the material internal friction coefficient α and the tool-chip friction angle β. The result is in agreement with Ye *et al*. (2012) solution for a slip-line field model for orthogonal cutting of pressure sensitive materials.

2.3.3 The average temperature rise on shear plane

The vast majority of energy consumption in the process of cutting is transformed into the cutting heat. The cutting heat is mainly originated from the plastic deformation work on the shear plane and the friction work of on the rake face. In order to calculate the cutting force, the temperature in Eq(8) and (9) must be obtained. However, it is difficult to use the experimental method to measure the temperature rise on shear plane directly. In this study a

method of assuming the shear work on shear plane is entirely transformed into heat is used to predict the temperature rise. The shear plane in our cutting model is considered as a closed plane heat source. The gross heat flows into the chip and the workpiece tool, but most of the heat is taken away by the chip with an inflow rate χ. Based on the above assumption and Lowen and Shaw's (1954) method, and combined with the orthogonal cutting geometry model, the expression for the average temperature rise can be written as

$$T_s = \frac{\chi \cdot \cos\gamma \cdot \cos(\varphi + \beta - \gamma) \cdot F_v}{c \cdot \rho \cdot t_1 \cdot w \cdot \cos(\varphi - \gamma) \cdot \cos(\beta - \gamma)} \tag{12}$$

where ρ is the material density, c is the specific heat capacity.

According to Lowen and Shaw's (1954), the inflow rate χ is as follows:

$$\chi = \frac{1}{1 + 1.33\sqrt{\dfrac{\xi \cdot \cos\gamma}{c \cdot \rho \cdot t_1 \cdot V \cdot \sin\varphi \cdot \cos(\varphi - \gamma)}}} \tag{13}$$

where ξ is the thermal conductivity.

Finally, the average temperature rise can be obtained by substituting the Eq(13) into Eq(12)

$$T_s = \frac{\cos\gamma \cdot \cos(\varphi + \beta - \gamma) \cdot F_v}{c \cdot \rho \cdot t_1 \cdot w \cdot \cos(\varphi - \gamma)\cos(\beta - \gamma)\left[1 + 1.33\sqrt{\dfrac{\xi \cdot \cos\gamma}{c \cdot \rho \cdot t_1 \cdot V \sin\varphi \cos(\varphi - \gamma)}}\right]} \tag{14}$$

3. Experimental validation of the model

3.1 Validation method

In order to validate the developed cutting model for BMG materials, cutting experiments were carried out. The cutting force analytical expressions (Eq(8) and (9)) contains the information of the M-C yield criterion, temperature, shear angle and the characteristics of geometric model etc. Therefore, cutting forces were measured and used to validate the cutting model.

3.2 Experiment design

The BMG workpiece used in the cutting experiments is a round bar of $Zr_{41.2}Ti_{13.8}Cu_{12.5}Ni_{10.0}Be_{22.5}$ (Vit1) alloy with 9.45mm in diameter and 90mm in length. The mechanical and physical properties of the workpiece material are listed in Table 1 are obtained from Inoue and Hashimoto (1998), Busch *et al*. (1995) and Bakkal *et al*. (2004). Cemented carbide cutting tools which have a cutting tool tip corner radius of 0.5mm, a tool rake angle γ = 4°, and a cutting edge angle κ_r =45°, were used. Similar to Li *et al* (2013)'s approach, the tool inclination angle θ was zero to ensure the orthogonal cutting condition in this paper. Limited by the preparation technique of metallic glasses, the rod workpiece was used in the cutting force validation experiment instead of large diameter disc as used in Li's experiments. In the experiment, a piezoelectric force dynamometer (Kistler 9119AA2) was used to measure the three mutually orthogonal cutting forces F_z, F_x and F_y, in the direction of cutting velocity, cutting tool feed velocity, and depth of cut respectively. In order to validate the model from a variety of cutting parameters, a fractional factorial experimental design with three factors and three levels was designed. Three controlled factors are spindle speed, feed rate and cutting depth and the parameter sets are listed in Table 2.

Table 1 The mechanical and physical properties of workpiece material Vit1

Material	T_g(K)	k(GPa)	α	ξ(W/m-K)	c(J/kg-K)	ρ(kg/m^3)	E(GPa)
Vit1	638	1	0.123	4	420	6125	96

The cutting force signals were measured during machining and chips were collected in the stable phase of turning process in each experiment. After the turning experiment, the chip thickness and chip width were measured by using a confocal laser scanning microscope, as shown in Fig.3(b).

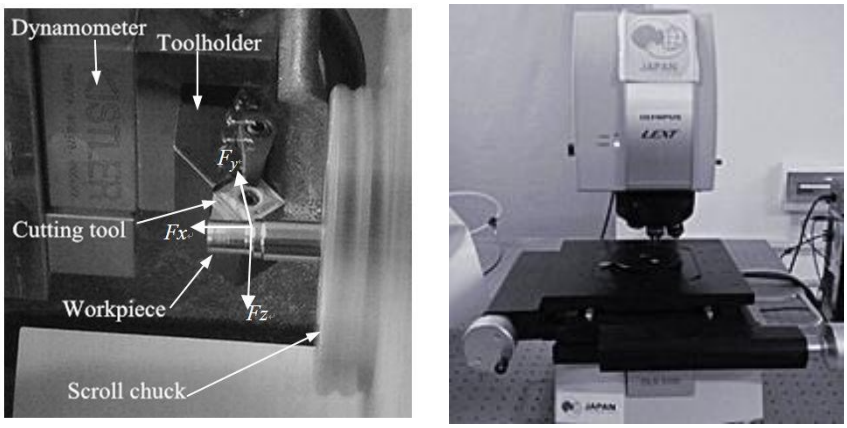

(a) (b)

Fig. 3 (a) the machining setup with dynamometer; (b) confocal laser scanning microscope (CLSM, OSL3100) to measure the chip thickness and the chip width.

Table 2. The results of turning experiments

No	Exp order	n-r/min	V-m/s	f-mm/r	a_p-mm	d_1-mm	d_2-mm	d-mm	δ-mm	Δ	F_x-N	F_y-N	F_z-N
1	7	160	0.068	0.08	0.1	8.22	8.10	0.06	0.040	0.40	22.7	88.0	55.3
2	4	160	0.078	0.1	0.2	9.44	9.16	0.14	0.060	0.30	62.5	149.5	106.1
3	1	160	0.077	0.12	0.3	9.45	8.93	0.26	0.040	0.13	79.8	139.2	121.1
4	5	250	0.118	0.08	0.2	9.16	8.85	0.16	0.045	0.23	59.7	136.5	91.6
5	2	250	0.114	0.1	0.3	8.93	8.43	0.25	0.050	0.17	85.8	148.3	116.2
6	8	250	0.105	0.12	0.1	8.10	7.98	0.06	0.040	0.33	16.3	55.4	35.2
7	3	400	0.172	0.08	0.3	8.43	7.95	0.24	0.060	0.20	71.2	124.2	94.9
8	9	400	0.158	0.1	0.1	7.60	7.48	0.06	0.040	0.40	18.4	78.3	46.3
9	6	400	0.182	0.12	0.2	8.85	8.53	0.16	0.040	0.33	50.6	119.4	88.0

(d_1 and d_2 are the workpiece diameters before and after turning by using vernier caliper, respectively. d is the actual cutting depth, $d=(d_1-d_2)/2$. δ is the cutting depth error, that is $\delta=a_p-d$. a_p is set by the machine in turning process)

3.3 Turning experiment results and analysis

The turning experiment results are shown in Table 2. In the cutting process we found,

although the overhang length of workpiece was not large, there was a relatively large error δ between the actual cutting depth d and the cutting depth a_p. The large error is mainly derived from the large elastic deformation of workpiece because of the small elastic modulus of BMG materials. Therefore, in order to obtain the accurate cutting depth, the workpiece diameters (d_1 and d_2) were measured before and after the turning experiments. For each point on the cutting edge with different cutting speeds, here, the cutting speed V was calculated from the midpoint along actual cutting depth (also is the midpoint of cutting edge contacted with workpiece).

Before the analysis of cutting force, a new parameter, Δ, is defined as the relative cutting depth error:

$$\Delta = \frac{\delta}{a_p} = \frac{a_p - d}{a_p} \tag{15}$$

where, δ is the cutting depth error and a_p is the theoretical cutting depth set by the machine. The relative cutting depth error Δ represents the degree of the elastic recovery on the machined surface and the deflection of workpiece rod. The value Δ can be obtained from each experiment and listed in Table 2. After comparison, the values Δ from the 3rd trial, 5th trial and 7th trial are smaller than others, the results are shown in Fig. 4.

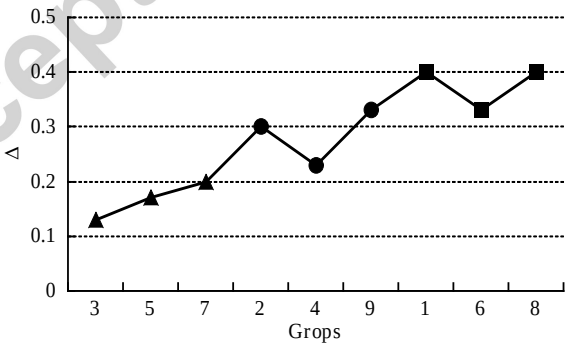

Fig. 4 The variation trend of Δ (▲a_p=0.3mm; ●a_p=0.2mm; ■a_p=0.1mm)

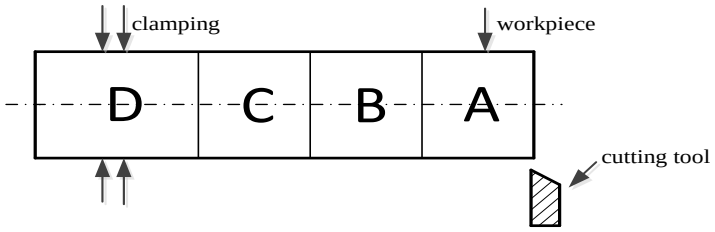

Fig.5 Three sections of the workpiece in experiments (A: a_p=0.3mm; B: a_p=0.2mm; C: a_p=0.1mm; D: clamping section)

9 cutting trials in Table2 were carried out by the sequence of cutting depth. The 3rd , 5th and 7th trials at the cutting depth 0.3mm were performed firstly in section A (shown in Fig.5), and then the 2nd, 4th and 9th trials were performed in section B. The 1st, 6th and 8th trials were performed in section C. This cutting order was to ensure the previous machined surface was not removed by the subsequent cuts.

In Fig.4, it can be seen that the relative cutting depth error Δ increases with the decrease of cutting depth a_p. The reason for larger relative cutting depth error at small cutting depth is because of that metallic glass has lower Young modulus although it has higher hardness. The proportion of elastic recovery to the cutting depth at 0.1 and 0.2mm is larger than that at 0.3mm. Therefore, the recovery cutting force caused by this phenomenon could not be ignored. Some factors, such as elastic recovery, tool edge radius, spindle speed and tool wear would influence the cutting depth error. The Vit1 metallic glass has both higher hardness and lower Young modulus, which is the main difference between the metallic glass and general crystalline metals. Because of its higher hardness, the Vit1 metallic glass is hard to machine and the tool wear takes place quickly. Compared with crystalline metals, the Vit1 workpiece generates larger elastic deformation at the same stress condition due to the lower Young modulus. A little ball made of Vit1 metallic glasses could bounce on the ground many times like a rubber ball. Therefore relatively larger elastic deformation caused by the lower Young modulus of Vit1 is believed to be the main factor for the cutting depth error.

After experiment, the tool surface was observed by CLSM in Fig.3(b) and it was found that, the contact area of the tool tip and workpiece on both rake and the flank face wore greatly, as shown in Fig.6. The 3rd, 5th and 7th trials of experiments were carried out firstly in all the

trials, the tool wear was not severe at that time, so the data of these trials are believed to be more reliable than others and were chosen for the force calculation. The tool wear observed from the Fig.6(c), can explain why the force component F_y is larger than the other two force components F_x and F_z in each experiment as shown in Table 2. In Fig.6(c), the severe tool wear of the transition area from flank face to vice flank face shows that the tool experiences large radial thrust force from workpiece because of the elastic recovery on the machined surface. The larger the force F_y is, the more this area wears.

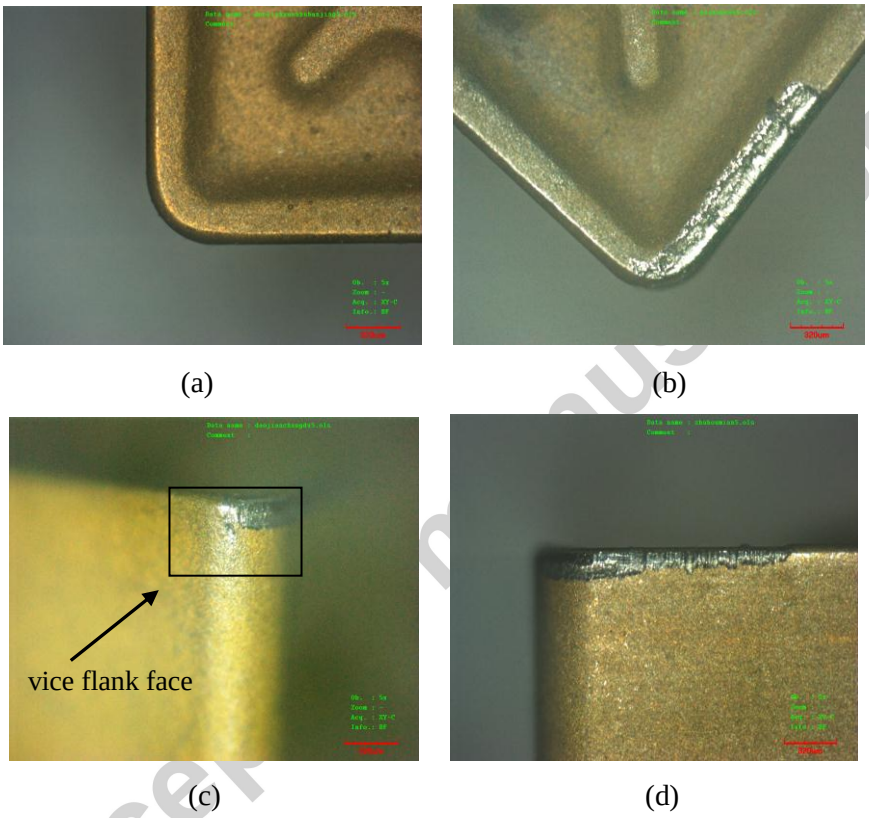

Fig. 6 Photographs of tool wear (a) The tool before using; (b) The rake face wear; (c) The wear of the contact parts of the tool tip and workpiece; (d) The flank wear.

The chip width w and chip thickness t_2 of the 3rd, 5th and 7th trials of experiment were measured by CLSM, shown in Fig.3(b) and the results are shown in Table 3.

Table 3 The information of chip, shear angle and (β-γ)

No	3rd	5th	7th

t_2(mm)	0.144	0.131	0.10
t_1(mm)	0.075	0.061	0.05
w(mm)	0.415	0.410	0.405
φ(°)	28.3	26	27.3
β-γ(°)	26.4	31	28.4

In order to obtain the other parameter values in Table 3, a two-dimensional sketch for turning process is established and shown in Fig.7. The a_p is replaced by the actual cutting depth d because of the influence of cutting depth error. The cutting thickness t_1 can be calculated by:

$$t_1 = \frac{f \cdot d}{w} \tag{16}$$

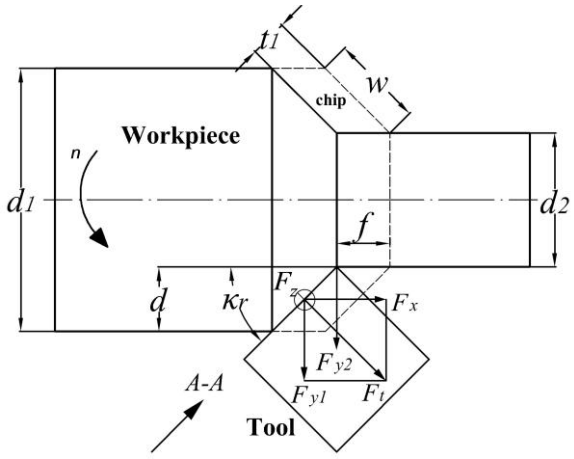

Fig. 7 The two-dimensional sketch for turning process

According to the geometric relationship in Fig. 1, the shear angle φ can be calculated by the known values of t_1 and t_2

$$\varphi = \arctan \frac{t_1 \cos \gamma}{t_2 - t_1 \sin \gamma} \tag{17}$$

Combining the Eq(11) and (17), the (β-γ) also can be obtained and the results are listed in Table 3.

3.4 Model validation and discussions

It is necessary to consider the force F_{y2} (shown in Fig.7) on the contact area of the tool tip and workpiece for the large elastic deflection deformation of workpiece. So the measured force F_y in table 2 can be decomposed into the two parallel force F_{y1} and F_{y2}. The geometrical model shown in Fig.1 does not include the force F_{y2} because the tool tip lies in the end of main cutting edge, which contacts the machined surface. In traditional cutting model, the elastic restoring force was ignored because it does not consider the contact effect between the tool tip, the flank and the machined surface. However, for the relative large elastic deformation, the cutting force F_{y2} in machining of Vit1, which comes from the tool tip and flank face, is not negligible. In fact, if the influence of the tool tip is not considered, the geometrical model shown in Fig.1 is quite consistent with the turning process seeing from the perspective *A-A* in Fig.7 when the tool edge inclination is zero. F_t is perpendicular to the direction of cutting velocity, and F_z is along the cutting direction (acting on the main cutting edge, perpendicular to F_x and F_y). Therefore the force relationship between the geometry model and the turning process can be established as follow:

$$F_p + N = F_t \tag{18}$$

$$F_v + f = F_z \tag{19}$$

where F_t is the resultant force of F_x and F_{y1}, $F_t=F_x/\cos\kappa_r$, and κ_r is the entering angle.

According to the previous assumption that the friction condition on the rake face and the flank face are assumed to be Coulomb friction, therefore, $f = N*\tan\beta$. It can be known from the geometrical relationship in Fig. 1, $F_p=F_v*\tan(\beta-\gamma)$. Using the Eq(18) and (19), finally the force F_v can be written as

$$F_v = \frac{F_z - \sqrt{2}\cdot\tan\beta\cdot F_x}{1-\tan\beta\cdot\tan(\beta-\gamma)} \tag{20}$$

Firstly the 3rd group of experimental data were used to calculate and compare the cutting forces of in Eq(8) and (20). By substituting the data in Table 2 and Table 3 for corresponding parameters in Eq(8), (14) and (20), the force F_v = 77.4N from Eq(20) and the force F_v=70.8N, which is the analytical value from Eq(8) were determined. Follow the same procedure, the 5th group and 7th group of experimental data are substituted and calculated. The three groups' comparison results of the analytical force values from Eq(8) and the measured forces value from Eq(20), are shown in Fig.8. The errors between the analytical value and the measured value are 8.5%, 9.4% and 5.3%, respectively, and the average error of them is 7.7%. The average temperature rise T_s calculated are 332.3K, 303.5K and 334.1K with the Eq(14), respectively. We take the T_0 as 293K, so the resultant temperature T are 625.3K, 596.5K and 627.1K respectively, which are under the glass transition temperature T_g. If the temperature is beyond T_g, the deformation mechanism is different from that at lower temperatures. The yield criterion Eq(1) will not be suitable beyond T_g because the metallic glass is temperature sensitive materials.

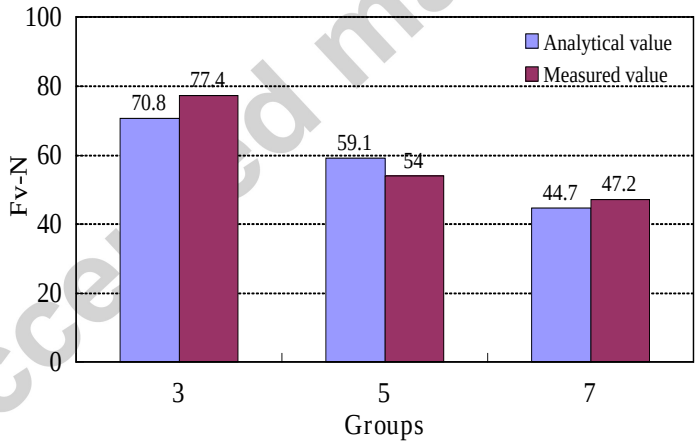

Fig. 8 The comparison results of the analytical forces and the measured forces.

Further, we make a comparison among the traditional analytical force expression, the analytical force expression without considering cutting temperature rise based on M-C criterion, our final expression in Eq(8) based on the M-C criterion and cutting temperature, and the measured force value in Eq(20). The traditional analytical force expression formulated by Merchant (1945b) is as follows:

$$F_v = \frac{k \cdot t_1 \cdot w \cdot \cos(\beta - \gamma)}{\sin\varphi \cdot \cos(\varphi + \beta - \gamma)} \tag{21}$$

And the analytical force expression without considering cutting temperature rise based on M-C criterion could be written as:

$$F_v = \frac{k \cdot t_1 \cdot w \cdot \cos(\beta - \gamma)}{[1 - \alpha \cdot \tan(\varphi + \beta - \gamma)] \cdot \sin\varphi \cdot \cos(\varphi + \beta - \gamma)} \tag{22}$$

The experiment data from the 3rd, 5th and 7th group are used and the comparison results are shown in Fig.9. The error between the traditional analytical force expression and the measured force value is more than 59%. The error between the analytical force expression for not considering cutting temperature rise based on M-C criterion and the measured force value is more than 73%. By comparing the above calculation results, it is clearly known that the cutting force value calculated from Eq(8) is closer to the measured value than others. Meanwhile it also indicates that the geometrical model we established is closer to the actual cutting process.

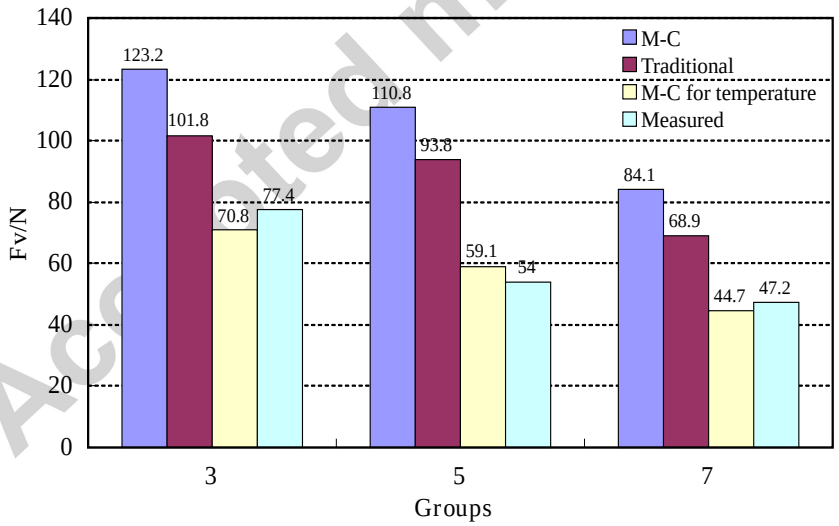

Fig. 9 Cutting force comparison between the three analytical force models and experiments

4. Concluding remarks

In this study, an orthogonal cutting geometry model of BMG was established considering the friction and pressure on the flank. The M-C yield criterion taking into account the influence

of normal stress and temperature was applied to the shear plane of the geometric model. The analytical expression for cutting force and shear angle were derived on the basis of the yield criterion and the geometric model.

The average temperature rise on shear plane also was calculated using the thermodynamic analysis method that the shear work on shear plane completely converted into heat, and the results show that the temperatures (concluding average temperature rise on shear plane and room temperature) are under the glass transition temperature of Vit1. This may be related to the minor cutting parameters in experiment.

In order to verify the cutting force expressions so the turning experiments were carried out. A minor average error of 7.7% between analytical value from the cutting force expression and the measured force value shows that the model has a high credibility. Among the three analytical cutting force models, the force value of the model based on M-C criterion and considering cutting temperature rise has the highest prediction accuracy.

Acknowledgment:

This work was sponsored by the National Natural Science Foundation of China (51105327), the Natural Science Foundation of Hebei Province (E2012203055) and the Engineering and Physical Sciences Research Council (EP/M020657/1). The authors are also grateful to Miss Rongjuan Yuan and Mr. Zhiyong Wang for their assistance in the work.

References

Bakkal, M., Shih, A.J., Scattergood, R.O., 2004. Chip formation, cutting forces, and tool wear in turning of Zr-based bulk metallic glass. Int. J. Mach. Tools Manuf. 44(9), 915-925.

Busch, R., Kim, Y. J., Johnson, W. L., 1995. Thermodynamics and kinetics of the undercooled liquid and the glass transition of the $Zr_{41.2}Ti_{13.8}Cu_{12.5}Ni_{10.0}Be_{22.5}$ alloy. J. Appl. Phys. 77 (8), 4039.

Chen, Y., Jiang, M.Q. and Dai, L.H. 2012. Temperature-dependent yield symmetry between tension and compression in metallic glasses. Acta Phys. Sin. 61(3), 1-6.

Fujita, K., Morishita, Y., Nishiyama, N., 2005. Cutting Characteristics of Bulk Metallic Glass. Mater. Trans.

46 (12), 2856-2863.

Inoue, A., Hashimoto, K., 1998, Amorphous and Nanocrystalline Materials, Berlin.

Jiang, M.Q., Dai, L.H., 2009. Formation mechanism of lamellar chips during machining of bulk metallic glass. Acta Mater. 57(9), 2730-2738.

Lee, J.C., Kim, Y.C., Ahn, J.P., Kim, H. S., 2005. Enhanced plasticity in a bulk amorphous matrix composite: macroscopic and microscopic viewpoint studies. Acta Mater. 53(1), 129–139.

Li, L.W., Li B., Li, X.C., Ehmann, K.F., 2013. Experimental investigation of hard turning mechanisms by PCBN tooling embedded micro thin film thermocouples. J. Manuf. Sci. Eng. Trans. ASME 135(4), 1-12

Liu, L.F., Dai, L.H., Bai, Y.L., Wei, B.C., Eckert, J., 2005. Behavior of multiple shear bands in Zr-based bulk metallic glass. Mater. Chem. Phys. 93(1), 174–177.

Lowen, E.G., Shaw, M.C., 1954. On the Analysis of Cutting-Tool Temperatures, Trans. ASME. 76, 217-231.

Lund, A.C., Schuh, C.A., 2004. The Mohr–Coulomb criterion from unit shear processes in metallic glass. Intermetallics. 12(10-11) , 1159–1165.

Merchant, M.E., 1945a. Mechanics of the metal cutting process II: plasticity conditions in orthogonal cutting, J. Appl. Phys. 16(5), 318-324.

Merchant, M.E., 1945b. Mechanics of the Metal Cutting Process. I. Orthogonal Cutting and a Type 2 Chip. J. Appl. Phys. 16(5), 267-275.

Sun, L., Jiang, M.Q., Dai, L.H., 2010. Intrinsic correlation between dilatation and pressure sensitivity of plastic flow in metallic glasse. Scripta Mater. 63(9),945-948.

Ye, G.G., Xue, S.F., Tong, X.H., Dai, L.H., 2012. Slip-line field modeling of orthogonal machining pressure sensitive materials. Int. J. Adv. Manuf. Tech. 58(9-12) , 907–914.

Zhang, Z.F., He, G., Eckert, J., Schultz, L., 2003a. Fracture Mechanisms in Bulk Metallic Glassy Materials. Phys. Rev. Lett. 91(4), 1-4.

Zhang, Z.F., Eckert, J., Schultz, L., 2003b. Difference in compressive and tensile fracture mechanisms of $Zr_{59}Cu_{20}Al_{10}Ni_8Ti_3$ bulk metallic glass. Acta Mater. 51(4), 1167–1179.

Development of an analytical model based on Mohr–Coulomb criterion for cutting of metallic glasses

Highlights

- A novel analytical cutting model based on Mohr-Coulomb yield criterion was developed, and the cutting temperature was considered in this analytical model.
- Orthogonal cutting experiments were performed on bulk metallic glasses $Zr_{41.2}Ti_{13.8}Cu_{12.5}Ni_{10}Be_{22.5}$.
- The results show that the model developed can accurately predict the cutting force and temperature.
- The average temperature rise calculated on shear plane was found under the glass transition temperature of $Zr_{41.2}Ti_{13.8}Cu_{12.5}Ni_{10}Be_{22.5}$.